Wood Sci Technol 37 (2003) 241–258
DOI 10.1007/s00226-003-0170-z

Original

A global model for the hot-pressing of MDF

L.M.H. Carvalho, M.R.N. Costa, C.A.V. Costa

Abstract The hot-pressing operation is the final stage in medium-density fiberboard (MDF) manufacture, where the mattress of fibers is compressed and heated to promote the cure of the resin. In MDF hot-pressing, many physical, chemical and mechanical processes are involved; the complexity of this operation arises from the fact that they are coupled. A global model is presented for this operation that integrates all mechanisms involved in the panel formation (heat and mass transfer, chemical reaction and mechanical behavior). This approach results in a two-dimensional unsteady state problem, which involves the knowledge of the polymerization kinetics of the resin, the transport properties and material properties, which are position and time dependent. This dynamic model was used to predict the evolution of the variables relating to heat and mass transfer (temperature, moisture content, gas pressure and relative humidity), as well as the variables relating to mechanical behavior (pressing pressure, strain, modulus of elasticity and density). The model performance was analyzed using the typical operating conditions for the hot-pressing of MDF and the results were compared to the experimental data from an industrial MDF press. We concluded that the model could predict in an acceptable way the behavior of the key variables for the control of the pressing cycle, as well as some physico–mechanical properties of the final product. The improvement of this model will permit the scheduling of the press cycle to fulfill objectives of

Received: 10 May 2001
Published online: 14 November 2003

L.M.H. Carvalho
Department of Wood Engineering, Polytechnic Institute of Viseu,
Campus Politécnico de Repeses, 3504-510 Viseu, Portugal

M.R.N. Costa
LSRE-Laboratory of Separation and Reaction Engineering,
Faculdade de Engenharia da Universidade do Porto,
Rua Roberto Frias, 4050–123 Porto, Portugal

C.A.V. Costa (✉)
LEPAE-Laboratory of Process, Environment and Energy Engineering, Faculdade de Engenharia da Universidade do Porto,
Rua Roberto Frias, 4050–123 Porto, Portugal
E-mail: ccosta@fe.up.pt
Fax: +351 225 081 449

This work was done under PRAXIS XXI research Project Number 2/2.1/TPAR/2079/95.

minimization of energy consumption, better quality of the board and increased process flexibility.

Abbreviations

Nomenclature

C_2	linear elastic constant
C_p	board specific heat (J kg^{-1} K^{-1})
C_{pg}	gas specific heat (J kg^{-1} K^{-1})
D_a	steam diffusivity in open air (m^2 s^{-1})
D_v	steam diffusivity in air within voids (m^2 s^{-1})
E	Young's modulus (MPa)
E	dimensionless Young's modulus
$\langle E \rangle$	overall Young's modulus (MPa)
Fo	Fourier number
Fo_m	Fourier number for mass transfer
h	heat transfer coefficient
Ho	dimensionless elastic number, (W m^{-2} K^{-1})
H	board moisture content (weight of water/weight of dry board)
H_i	board initial moisture content
HR	relative humidity
ΔH_r	resin polycondensation enthalpy (J/kg)
k	thermal conductivity (W m^{-1} K^{-1})
k_c	mass transfer coefficient for steam (m s^{-1})
K_g	board permeability to gas phase (m^2)
L_r	board radius (m)
L_z	board half-thickness (m)
$\dot{m}$	mass of water evaporated per unit volume and time (kg s^{-1} m^{-3})
MM_a	air molecular weight (kg $kgmol^{-1}$)
MM_w	water molecular weight (kg $kgmol^{-1}$)
N_p	relative permeability
N_z	total number of points along z-coordinate
Nu	Nusselt number
P	dimensionless pressure
P	total gas pressure (N m^{-2})
P_∞	ambient pressure, (N m^{-2})
Pe	Peclet number for heat transfer
Pe_m	Peclet number for mass transfer
P_{sat}	saturated vapor pressure (N m^{-2})
P_v	steam partial pressure (N m^{-2})
P_v	dimensionless steam partial pressure
Q_l	heat of desorption (J kg^{-1})
$(-r)$	reaction rate for resin polycondensation (s^{-1})
$\Re$	gas constant (8.314 kJ $kgmol^{-1}$ K^{-1})
R	dimensionless radial coordinate
Sh	Sherwood number
t	time after press closure (s)
T	temperature (K)
T	dimensionless temperature
T_p	platen temperature (K)
T_∞	ambient temperature (K)

T_g glass transition temperature (K)
Vi dimensionless viscoelastic number
V volume fraction
v_g velocity of gas phase (m s^{-1})
y_{res} resin content (weight of resin/dry fiber weight)
z spatial variable (distance along z-coordinate)
Z Dimensionless spatial variable

Greek symbols
ϵ strain
ϵ_p board porosity (m^3 mat void/m^3 dry mat)
α adhesive degree of cure
λ heat of vaporization of water (J kg^{-1})
μ viscous component (Pa s)
μ dimensionless viscous component
$\langle\mu\rangle$ overall viscous component (Pa s)
μ_g gas viscosity (Ns m^{-2})
ρ density (kg m^{-3})
ρ_c oven-dry board density (kg m^{-3})
ρ_f oven-dry fiber density (kg m^{-3})
ρ_s solid (resin+wood) material density (kg m^{-3})
σ compression stress (MPa)
ϕ flux (kg m^{-2} s^{-1})
τ press cycle time (s)
θ dimensionless time variable

Subscripts
a air
c composite
f fiber
g gas
0 reference
r radial coordinate (from the center of the board)
s solid
v steam
w water
z vertical coordinate along the thickness of the board (from the center of the board)

Introduction

Medium-density fiberboard (MDF) is a wood-based sheet material manufactured from wood fibers bonded together with a synthetic resin adhesive (Maloney 1989). The consolidation of wood fiber mats is achieved by a hot-pressing process. Several types of hot-presses can be used: batch or continuous, steam injection, radio-frequency or microwaves. This process is quite complex since it involves simultaneous and coupled heat and mass transfer, polymerization of the adhesive and forming. A better understanding and possibly optimization and control of this operation can be achieved through simulation using physical models.

The work on this field is very scarce, even for other wood-based panels like particleboard. The first models that were developed for the hot-pressing of par-

ticleboard attempted to describe only simultaneous heat and mass transfer. Most of them were one-dimensional and considered only the thickness direction (Kamke and Wolcott 1991). The improvement of computer performance aided the development of two- or three-dimensional models, although with some limiting simplifications, namely treating the problem as pseudo-steady state (Humphrey and Bolton 1989), or predicting only the behavior of a single variable (Hata et al. 1990). For MDF, a three-dimensional unsteady state model was presented (Carvalho and Costa 1998) describing the heat and mass transfer and predicting the spatial and time evolution of temperature, moisture content, steam pressure and relative humidity.

The rheological behavior of the mattress during pressing involves complex phenomena that are tightly coupled with temperature and moisture content distributions. On the other hand, the density profile affects the heat and steam fluxes across the mat porous structure. The theoretical description of this mechanism during the pressing of wood-based panels has been published in several publications, mostly for particleboard, although a few models attempted to include the heat and mass transfer (Harless et al. 1987; Suo and Bowyer 1994). Most models are restricted to the description of the stress–strain behavior, and the viscoelastic response is not considered (Dai and Steiner 1993; Lenth and Kamke 1996; Lang and Wolcott 1996). In the case of MDF, we proposed a mechanical model (Carvalho et al. 2001) to describe the viscoelastic behavior of this material, which was used as input. The data predicted by the three-dimensional heat and mass transfer model were previously developed. The model was used to predict the evolution of compression stress, strain, modulus of elasticity and density with time at a given position in the mattress, as well as the density profiles.

Recently, the model developed by Humphrey(1982) for the hot-pressing of particleboard in a batch press has been improved and extended to the continuous process (Thoemen and Humphrey 1999). However, this model ignores the influence of the resin cure.

Taking into account the work already done on developing comprehensive and predictive models for the hot-pressing of MDF, the understanding, optimization and control of this operation requires further investigations. The relationship between manufacturing variables and physical–mechanical properties demands an improvement of models in order to integrate all the mechanisms involved. The objectives of this work are:

- To develop and present a global model for the MDF cure in a batch hot press, which includes simultaneously heat and mass transfer, polymerization reaction and rheology. The influence of the resin cure is included not only in the rheological behavior, which is affected by the adhesive bond strength development, but also in the heat and mass transfer, because the resin polycondensation reaction is exothermic and produces water.
- To show the simulation capabilities of the model in a fairly large range of parameter space.
- To compare simulation results with a few experimental points obtained in an industrial press.

Model development and numerical solution

In order to simplify the numerical solution of the global model, we considered a cylindrical board, with cylindrical and vertical symmetry. The simulation results obtained with 2D and 3D heat and mass transfer models indicated that the

simplified model allows a very accurate description of the profiles and time evolution, except for the edges (Carvalho and Costa 1997). This problem can be overcome by considering an interpolation using the two cylindrical forms inscribed and circumscribed to the rectangular board. So, we present the equations for the cylindrical board and only the top of half of the board was modelled.

In model construction we made the following assumptions:

1. The consolidation of the fiber mattress occurs in a vertical direction, and no lateral expansion is considered since it is quite small, practically not affecting thickness reduction and mass and heat flow through the lateral surface.
2. Viscoelastic behavior during the whole press-cycle.
3. Position control during the press cycle: a perturbation in thickness (or total strain) is imposed and the response in stress is observed as it is commonly done in industrial presses.
4. Two phases (solid phase and gaseous phase) are considered and a local thermodynamic equilibrium is assumed. Any resistance to heat and mass transfer between the gas phase and the adjacent solid phase is neglected; in fact, the fibers are always below their saturation point and so there is no liquid water (Humphrey and Bolton 1989; Carvalho and Costa 1998). On the other hand, most drying processes are slow and particle sizes and pore diameters are small when compared to the characteristic lengths of the system (Silva 2000).
5. The bound water in fibers is in equilibrium with the gas (air+steam) in voids. The moisture content and relative humidity obey a sorption isotherm at the local temperature.
6. The total heat supply to the mattress comes from the heated press platens and from the exothermic curing reaction of the resin binder. The heat of compression of the mattress is neglected (Humphrey 1982).
7. The water produced by the condensation reactions of resin binder is included.
8. The convective flow of the gas phase follows Darcy's law.
9. The gas mixture follows the ideal gas law.
10. Physical properties in each mattress position are all dependent on temperature, wood moisture content and steam pressure at the point in question in the mattress. Transport properties, which are dependent on changing physical properties, can also vary with respect to space and time. At the same vertical position, the properties along the same radius are equal.
11. – Conduction of heat between the hot platens and the central layer of the mattress (the heat transferred by radiation is likely to be insignificant compared to the conduction at temperatures as low as the typical platen temperature).
    – Phase change of water from the adsorbed to the vapor state.
    – Convective heat and mass transfer.
12. Although it is possible that vitrification or plastification of wood can occur on the surfaces close to the platen, no additional resistance to heat and mass transfer at the platen is considered.

In the global model, the following dependent variables were considered:

- For heat and mass transfer: temperature, steam partial pressure, gas pressure (air+steam) and mattress moisture content.
- For mechanical behavior: vertical position, overall compressive stress and the following set of equations.

- For heat and mass transfer: two mass balances (one for the gas mixture and the other for steam), one energy balance and one equilibrium equation for the moisture sorption isotherm.
- For mechanical behavior: one equation for the calculation of the overall elasticity modulus from every local elasticity moduli, one equation for the overall viscous component from every local viscous components, one equation that relates the vertical position and local strain, and finally the Maxwell model to calculate the overall stress. The top half of the board was divided into N_r rings, each with N_z layers, where the rings have the same overall strain. The strain on every control volume is also calculated considering the Maxwell model.

When the mattress of fibers is subjected to a mechanical pressure, the board thickness and the vertical position z will change with time. In order to fix the domain of integration, we adopted a transformation introduced by Landau (Landau and Lewis 1950)

$$Z = \frac{z}{L_z(t)} \tag{1}$$

We considered the following variables and parameters that will appear in the constitutive model equations:

$$R = \tfrac{r}{L_r},\quad L_z = \tfrac{L_z}{L_{z0}},\quad R_r = \tfrac{L_{z0}}{L_r},\quad \theta = \tfrac{t}{\tau},\quad \Delta Z_{i,j,k} = \tfrac{\Delta z_{i,j,k}}{L_z\,L_{z0}},\quad \Delta Z_0 = \tfrac{\Delta z_0}{L_{z0}} = \tfrac{1}{N_z},\quad \sigma_T = \tfrac{\sigma_T}{\sigma_{T0}},$$
$$E_{i,j,k} = \tfrac{E_{i,j,k}}{E_0},\quad \mu = \tfrac{\mu}{\mu_0},\quad \rho_{c0} = \tfrac{\rho_c}{\rho_{c0}},\quad \varepsilon_p = \tfrac{\varepsilon_p}{\varepsilon_{p0}},\quad T = \tfrac{T-T_\infty}{T_0-T_\infty},\quad P = \tfrac{P}{P_0},\quad P_v = \tfrac{P_v}{P_0},\quad \rho_g = \tfrac{\rho_g}{\rho_{g0}},$$
$$C_p = \tfrac{C_p}{C_{p0}},\quad C_{pg} = \tfrac{C_{pg}}{C_{pg0}},\quad k_x = \tfrac{k_x}{k_{0z}},\quad k_z = \tfrac{k_z}{k_{0z}},\quad \nu_{gr} = \tfrac{\nu_{gr}}{\nu_{g0z}},\quad \nu_{gz} = \tfrac{\nu_{gz}}{\nu_{g0z}},\quad D_{vr} = \tfrac{D_{vr}}{D_{v0z}},$$
$$D_{vz} = \tfrac{D_{vz}}{D_{v0z}},\quad K_{gr} = \tfrac{K_{gr}}{K_{g0z}},\quad K_{gz} = \tfrac{K_{gz}}{K_{g0z}},\quad \mu_g = \tfrac{\mu_g}{\mu_{g0}},\quad h = \tfrac{h}{h_0},\quad k_c = \tfrac{k_c}{k_{c0}},$$

where σ_{T0}, E_0, ρ_{g0}, C_{p0}, k_{0z}, C_{pg0}, D_{v0z}, ν_{g0z}, K_{g0z}, μ_{g0} are the reference properties described in nomenclature; P_0 is the initial total pressure and T_0 is equal to the platen temperature (T_p), which is constant. Here L_{z0} is the initial board half-thickness, and τ is the press cycle time. The dimensionless numbers are

$$Ho = \frac{E_0}{\sigma_0},\qquad Vi = \frac{E_0\tau}{\mu_0},\qquad Fo_z = \frac{\tau\,k_{0z}}{\rho_{c0}\,C_{p0}\,L_{z0}^2},\qquad Pe_z = \frac{\rho_{g0}\,C_{pg0}\,\nu_{g0z}\,L_{z0}}{k_{0z}},$$
$$Pe_r = \frac{Pe_z}{R_r},\qquad Fo_{mz} = \frac{\varepsilon_{p0}\,D_{v0z}\tau}{L_{z0}^2},\qquad Pe_{mz} = \frac{\nu_{g0}\,L_{z0}}{\varepsilon_{p0}\,D_{v0z}},\qquad Pe_{mr} = \frac{Pe_{mz}}{R_r},$$
$$N_{pz} = \frac{P_0\,K_{g0z}\,\tau}{\varepsilon_{p0}\,\mu_{g0}\,L_{z0}^2},\qquad Nu_r = \frac{h_0\,L_r}{k_{0z}} = \frac{Nu_z}{R_r},\qquad Sh_r = \frac{k_{c0}\,L_r}{D_{v0z}} = \frac{Sh_z}{R_r}.$$

The following parameters were also considered, where $\dot{m}$ is the mass of water evaporated per unit volume and time:

$$\dot{M} = \frac{\dot{m}\,\tau}{\rho_{c0}},\qquad \dot{M}_v = \frac{\dot{m}\,\tau}{\rho_{v0}\varepsilon_{p0}},\qquad \dot{M}_g = \frac{\dot{m}\,\tau}{\rho_0\,\varepsilon_{p0}},$$

where

$$\rho_{v0} = \frac{MM_w P_0}{\Re(T_0 - T_\infty)},\qquad \rho_0 = \frac{MM_a P_0}{\Re(T_0 - T_\infty)}.$$

The velocities of the gas phase for each direction are calculated using Darcy's law (with no gravitational effect)

$$v_{gr} = -\frac{K_{gr}}{\mu_g}\frac{\partial P}{\partial r}, \qquad v_{gz} = -\frac{K_{gz}}{\mu_g}\frac{\partial P}{\partial z},$$

where K_{gz} and K_{gr} are the board permeabilities in the z- and r-directions, respectively, μ_g is the viscosity of the gas phase and P the total gas pressure.

The cure reaction is also considered for heat and mass transfer. In the energy balance we included a term for the energy released by the cure reaction, where $(-r)$ is the reaction rate in s^{-1} and ΔH_r the enthalpy of the polycondensation reaction. In the mass balance we included the water produced during the polycondensation reaction, where $(-r')$ is the reaction rate expressed in kilograms of water per kilogram of resin per second.

Before the presentation of the constitutive equations in dimensionless form, it is important to mention that due to the inclusion of Landau transformation (1950) in spatial variable z (see Eq. (1)), the time derivative of a variable Ψ could be expressed by the following expressions:

$$\left(\frac{\partial \psi}{\partial \theta}\right)_Z = \left(\frac{\partial \psi}{\partial z}\right)_t \cdot \left(\frac{\partial z}{\partial \theta}\right)_Z + \left(\frac{\partial \psi}{\partial t}\right)_z \cdot \left(\frac{\partial t}{\partial \theta}\right)_Z,$$
$$\left(\frac{\partial \psi}{\partial t}\right)_z = \frac{1}{\tau}\left(\frac{\partial \psi}{\partial \theta}\right)_Z - \frac{Z}{\tau}\frac{\dot{L}_z}{L_z}\left(\frac{\partial \psi}{\partial Z}\right)_t, \tag{2}$$

where

$\dot{L}_z$

is the rate of the boundary (board half-thickness).

For a two-dimensional problem, the energy balance in dimensionless form is given by the following equation:

Energy balance

$$\frac{\partial T}{\partial \theta} = -\frac{Fo_z}{\rho_c C_p}\left[\frac{R_r^2}{R}\frac{\partial (R\varphi_{tr})}{\partial R} + \frac{1}{L_z}\frac{\partial \varphi_{tz}}{\partial Z}\right] - \frac{\dot{M}(\lambda + Q_l) + (-r)\left(\frac{\gamma_r}{1+\gamma_r}\right)\Delta H_r \rho_c \tau}{\rho_c C_p C_{p0}(T_0 - T_\infty)} + Z\frac{\dot{L}_z}{L_z}\frac{\partial T}{\partial Z},$$
$$\varphi_{tr} = -k_r\frac{\partial T}{\partial R} + \frac{Pe_z}{R_r}\rho_g C_{pg} v_{gr}\left(T + \frac{T_\infty}{T_0 - T_\infty}\right),$$
$$\varphi_{tz} = -\frac{k_z}{L_z}\frac{\partial T}{\partial Z} + Pe_z \rho_g C_{pg} v_{gz}\left(T + \frac{T_\infty}{T_0 - T_\infty}\right), \tag{3}$$

with the following initial and boundary conditions:

$$\text{IC}: \quad T(R, Z, 0) = 0, \tag{4}$$

$$\text{BC}: \quad \left.\frac{\partial T}{\partial R}\right|_{R=0} = 0, \quad \left.\frac{\partial T}{\partial Z}\right|_{Z=0} = 0, \quad T(R,1,\theta) = 1, \quad T(1,Z,\theta) = 0. \tag{5}$$

Alternatively, considering an external resistance to heat transfer through the board edges

$$-k_r \left.\frac{\partial T}{\partial R}\right|_{R=1} = Nu_r\, h\, T|_{R=1}. \tag{6}$$

The mass conservation equation for steam in dimensionless form is given by

Mass balance (steam)

$$\dot{M}_\text{v} = Fo_\text{mz}\left[\varepsilon_\text{p}\frac{R_r^2}{R}\frac{\partial(R\,\varphi_\text{vr})}{\partial R} + \frac{1}{L_z}\frac{\partial\left(\varepsilon_\text{p}\,\varphi_\text{vz}\right)}{\partial Z}\right],$$

$$\varphi_\text{vr} = -D_\text{vr}\frac{\partial}{\partial R}\left(\frac{P_\text{v}}{T+\frac{T_\infty}{T_0-T_\infty}}\right) + \frac{Pe_\text{mz}}{\varepsilon_\text{p}\,R_r}\nu_{gr}\left(\frac{P_\text{v}}{T+\frac{T_\infty}{T_0-T_\infty}}\right), \tag{7}$$

$$\varphi_\text{vz} = -\frac{D_\text{vz}}{L_z}\frac{\partial}{\partial Z}\left(\frac{P_\text{v}}{T+\frac{T_\infty}{T_0-T_\infty}}\right) + \frac{Pe_\text{mz}}{\varepsilon_\text{p}}\nu_\text{gz}\left(\frac{P_\text{v}}{T+\frac{T_\infty}{T_0-T_\infty}}\right),$$

$$\frac{\partial P_\text{v}}{\partial\theta} = -\frac{\left[\dot{M} + (-r')\left(\frac{y_r}{1+y_r}\right)\rho_\text{c}\,\tau\right]}{\rho_\text{c}\left(\frac{\partial H}{\partial HR}\right)_T\frac{P_0}{P_\text{sat}}} + Z\frac{\dot{L}_z}{L_z}\frac{\partial P_\text{v}}{\partial Z}, \tag{8}$$

where the relative humidity is calculated from
$HR = \frac{P_\text{v}}{P_\text{sat}}$

$$\text{IC}: \quad P_\text{v}(R,Z,0) = P_\text{v}(H = H_i; T = 0), \tag{9}$$

$$\begin{aligned}\text{BC}: \quad & \left.\frac{\partial P_\text{v}}{\partial R}\right|_{R=0} = 0, \quad \left.\frac{\partial P_\text{v}}{\partial Z}\right|_{Z=0} = 0,\\ & P_\text{v}(1,Z,\theta) = P_\text{v}(H = H_i; T = 0),\\ & \left.\frac{\partial P_\text{v}}{\partial Z}\right|_{Z=1} = 0.\end{aligned} \tag{10}$$

Alternatively, considering an external resistance to mass transfer through the board edges

$$-D_\text{vr}\frac{\partial}{\partial R}\left(\frac{P_\text{v}}{T+\frac{T_\infty}{T_0-T_\infty}}\right)\Bigg|_{R=1} = Sh_r\,k_\text{c}\left(\frac{P_\text{v}|_{R=1}}{T+\frac{T_\infty}{T_0-T_\infty}} - \frac{P_\text{v}(H = H_i; T = 0)}{\frac{T_\infty}{T_0-T_\infty}}\right). \tag{11}$$

The mass conservation equation for the gas mixture (air+steam) can be written in dimensionless form as

Mass balance (gas mixture: air+steam)

$$\frac{\partial P}{\partial \theta} = -\frac{N_{pz}}{\varepsilon_p}\left[\frac{R_r^2}{R}\frac{\partial\left(R\varphi_{gx}\right)}{\partial R} + \frac{\partial \varphi_{gz}}{\partial Z}\right]\left(T + \frac{T_\infty}{T_0 - T_\infty}\right) + \frac{\dot{M}_g}{\varepsilon_p}\left(T + \frac{T_\infty}{T_0 - T_\infty}\right) + \frac{P}{\left(T + \frac{T_\infty}{T_0 - T_\infty}\right)}\frac{\partial T}{\partial \theta} + Z\frac{\dot{L}_z}{L_z}\left[\frac{\partial P}{\partial Z} - \frac{P}{\left(T + \frac{T_\infty}{T_0 - T_\infty}\right)}\frac{\partial T}{\partial Z}\right],$$

$$\varphi_{gr} = -\frac{K_{gr}}{\mu_g}\frac{P}{\left(T + \frac{T_\infty}{T_0 - T_\infty}\right)}\frac{\partial P}{\partial R},$$

$$\varphi_{gz} = -\frac{K_{gz}}{\mu_g L_z}\frac{P}{\left(T + \frac{T_\infty}{T_0 - T_\infty}\right)}\frac{\partial P}{\partial Z}. \tag{12}$$

$$\text{IC}: \quad P(R, Z, 0) = \frac{P_\infty}{P_0}, \tag{13}$$

$$\text{BC}: \quad \left.\frac{\partial P}{\partial R}\right|_{R=0} = 0, \quad \left.\frac{\partial P}{\partial Z}\right|_{Z=0} = 0, \quad P(1, Z, \theta) = \frac{P_\infty}{P_0}, \quad \left.\frac{\partial P}{\partial Z}\right|_{Z=1} = 0. \tag{14}$$

For viscoelastic behavior, the equations in dimensionless form are
Viscoelastic behavior

$$\frac{\partial \sigma_T}{\partial \theta} = Ho\,\langle E\rangle\,\frac{\partial L_z}{\partial \theta} - Vi\frac{\langle E\rangle}{\langle \mu\rangle}\sigma_T, \tag{15}$$

$$\langle E\rangle = \frac{1}{N_r}\sum_i E_i, \qquad E_i = \frac{1}{\Delta Z_0}\frac{1}{\sum_{k=1}^{N_z}\frac{1}{E_{i,k}}}, \tag{16}$$

$$\langle \mu\rangle = \frac{1}{N_r}\sum_i \mu_i, \qquad \mu_i = \frac{1}{\Delta Z_0}\frac{1}{\sum_{k=1}^{N_z}\frac{1}{\mu_{i,k}}}, \tag{17}$$

$$\text{IC}: \quad \sigma_T = 0, \qquad L_z(\theta) = 1, \tag{18}$$

$$\frac{\partial Z_{i,k}}{\partial \theta} = \frac{\Delta Z_0}{2L_z}\left(\frac{\partial \varepsilon_{i,k}}{\partial \theta} + 2\sum_{l=1}^{k-1}\frac{\partial \varepsilon_{i,k}}{\partial \theta}\right) - \frac{Z_{i,k}}{L_z}\frac{\partial L_z}{\partial \theta}, \tag{19}$$

$$\frac{\partial \varepsilon_{i,k}}{\partial \theta} = \frac{1}{Ho\, E_{i,k}}\frac{\partial \sigma_T}{\partial \theta} + \frac{Vi}{E_0}\frac{\sigma_T}{\mu_{i,k}}, \tag{20}$$

$$\text{IC}: \quad Z_{i,k} = \frac{K - 0.5}{N_z}, \qquad \varepsilon_{i,k} = 0. \tag{21}$$

Density and porosity are calculated using the following equations:

$$\rho_{c_{i,k}} = \frac{\Delta Z_0}{\Delta Z_{i,k}\, L_z}, \tag{22}$$

$$\varepsilon_{p_{i,k}} = \frac{1}{\varepsilon_{p0}}\left(1 - \frac{\rho_{i,k}\,\rho_{c0}}{\rho_s}\right), \tag{23}$$

with

$$\Delta Z_{i,k} = 2\left(Z_{i,k} - \sum_{l=1}^{k-1}\Delta Z_{i,l}\right).$$

The physical and transport properties were estimated using several correlations from literature (Carvalho and Costa 1998). In the absence of models for wood sorption isotherms that perform well in the range of temperatures observed in the hot-pressing, we fitted the data from Kauman (1956) using cubic spline interpolation (De Boor 1978). To estimate the local elastic properties we used the micromechanical model PPP, which consists of three springs in series corresponding to the three elements involved (fiber+resin+gas, Carvalho et al. 2001). So, to calculate the composite modulus of elasticity, a longitudinal rule of mixtures was used combined with the relationships derived for "honeycomb-type" cellular structures (Gibson and Ashby 1988). We concluded in a previous work (Carvalho et al. 2001) that this solution is fairly effective in predicting the influence of the porous structure density during compression. The expression is

$$E_c = C_2\, E_s\left(\frac{\rho_c}{\rho_s}\right)^3 + E_g\left(1 - \frac{\rho_c}{\rho_s}\right), \tag{24}$$

where C_2 is a linear elastic constant equal to 0.05. The elastic modulus of the solid E_s (fiber+resin) can be calculated using the longitudinal rule of mixtures

$$E_s = V_f\, E_f + V_{res}\, E_{res}, \tag{25}$$

where E_f and E_{res} are the Young's moduli of the fiber and resin, respectively, and V_f and V_{res} are the fiber and resin volume fractions, respectively. The fiber and resin Young's moduli were calculated using experimental data from literature (Carvalho 1999), taking into account the influence of the temperature and moisture content for the fiber and the temperature and time for the resin

hardening. The elasticity modulus of the gas mixture E_g (steam+air) entrapped in voids can be calculated by

$$E_g = \frac{P - P_0}{\varepsilon}. \tag{26}$$

The temperature dependence of the viscous component for the wood–resin model was estimated using an Arrhenius-type equation

$$\mu = \mu_\infty \exp\left(\frac{\Delta E_\mu}{\Re T}\right), \tag{27}$$

with the following parameters (Carvalho et al. 2001): μ_∞=1×10^8 Pa s, and ΔE_μ=3,241 J/mol.

The kinetic model for the UF resin polycondensation reaction was obtained in a previous work using Raman spectroscopy (Carvalho 1999). It was concluded that the evolution of the bands attributed to methylene groups follows first-order kinetics. Although the cross-linking is mainly obtained by the formation of methylene bridges, other reactions, such as the formation of cyclic structures or methylene–ether bridges, are also involved. However, as a good approximation, we can consider the kinetics of the formation of methylene bridges B representative of the polycondensation kinetics. So, the rate of the polycondensation reaction of UF resin (in s^{-1}) can be calculated using

$$(-r) = \frac{1}{A_0}\frac{\mathrm{d}[B]}{\mathrm{d}\,t} = \frac{1}{2}k\ \exp(-k\,t), \tag{28}$$

where A_0 is the initial concentration of methylol groups, and k is the rate constant calculated using the Arrhenius equation with k_0=71.597 s^{-1} and E_{act}=33 kJ/mol. The water production by the polycondensation reaction was calculated, keeping in mind that for each methylene bridge formed a water molecule is released. We can calculate the water production in kilograms of water per kilogram of resin per second with the expression

$$(-r') = \frac{\mathrm{d}\,[-H_2O]}{\mathrm{d}\,t} = \frac{1}{2}\ A_0\,k\ \exp(-k\,t)\ MM_w. \tag{29}$$

Using data obtained in a quantitative ^{13}C-NMR analysis, we obtained A_0 = 7.9 mol/kg.

To calculate the heat released by the resin cure reaction, the polycondensation enthalpy (ΔH_r) for the UF resin is needed. For that, we took ΔH_r=84.13 J/g of resin obtained by Yin (1994) using DSC for a UF resin with 1.5% (w/w) of hardener (NH_4Cl), which is the typical hardener content used in MDF production.

Numerical method

This approach results in a nonlinear unsteady state two-dimensional problem, which was numerically solved using the method of lines. The variables were discretized in space by finite differences (Patankar 1980), and the resulting set of initial value differential equations was handled using the special stiff equations solver LSODES (Hindmarsh 1983). This solver uses the Gear method and treats

the Jacobian matrix in general sparse form to avoid the computation of zero-valued Jacobian entries. The time derivatives of temperature, gas pressure and steam partial pressure demanded the use of spatial discretization, which followed the control volume approach. The control volume consists of concentric rings, the same grid as outlined by Carvalho and Costa (1997); the discretization follows the radial direction and the vertical direction (board thickness). The parameters of LSODES were set according to the instructions. The Jacobian matrix was computed internally, and we set the relative error to 1×10^{-6} and absolute error to 1×10^{-8}.

Experimental data

The experimental data for model predictions comparison was supplied by a Portuguese manufacturer of MDF and it was obtained in an industrial batch MDF hot press. Temperature was measured with a K-type thermocouple positioned at the mat center. The press control system provides the position of the top platen and the pressure in the hydraulic system.

Results and discussion

The global model was used to predict the evolution of the variables related to heat and mass transfer (temperature, moisture content, gas pressure and relative humidity), as well as the variables related to mechanical behavior (pressing pressure, strain, modulus of elasticity and density). Several simulations were carried out to show the ability of the model to perform well in a fairly large range of parameter values. First, we present the results for a set of typical operating conditions: platen temperature=190 °C, press cycle time=330 s, board final thickness=19 mm, board radius=4.39 m, initial moisture content=11%, resin content=8.5% and final board density=750 kg/m^3. Finally, we present the comparison between the simulation results with a few experimental results obtained in the industrial press.

Figure 1 displays the evolution of pressing pressure, viscous component and modulus of elasticity with time at a given position in the mattress, as well as the time evolution of the density profiles. The time is counted from the moment when the top platen touches the top surface of the mat. The model performance was examined, imposing the perturbation in the board thickness represented in Fig. 1a. Previous analysis (Carvalho et al. 2001; Carvalho 1999) of the influence of several parameters, such as the platen temperature or the board moisture content, on its mechanical behavior gave results that are perfectly in agreement with those obtained with the global model using the same perturbation and the same micromechanical model.

Figure 2 shows plots of the dependent variables as a function of time at the central horizontal plane of the mattress using the thickness position as a parameter. On each plot the curves are numbered from 1, adjacent to the board mid-plane, to 10, adjacent to the board surface.

In this figure we can see the effect of board compression on heat and mass transfer. The results are qualitatively similar with those obtained assuming instantaneous closing of the press and no densification of the mat (Carvalho and Costa 1998). The rate of temperature rise is higher at surface layers, because the core temperature is affected less by the platen temperature. However, a delay is observed in this temperature rise, mostly in the central layers. As a consequence, the moisture content is higher at the end of the press cycle. The decrease in mat porosity gives rise to an important increase in gas pressure that is not balanced by

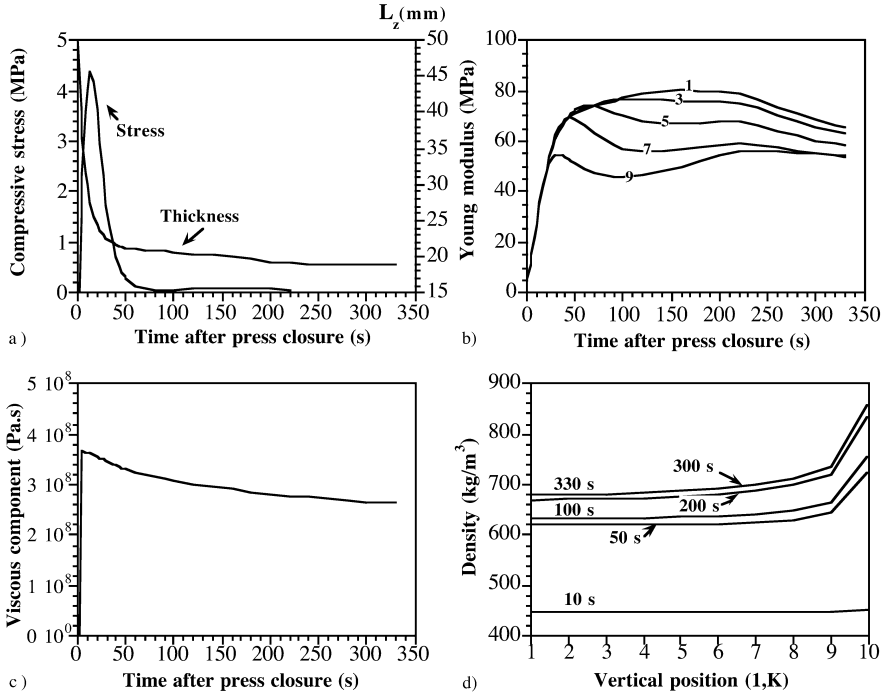

Fig. 1. Evolution of: **a** Overall compressive stress. **b** Young's modulus. **c** Viscous component with time after press closure for several positions in the vertical direction (*numbered from 1*, adjacent to board mid-plane, *to 10*, adjacent to board surface). **d** Vertical profiles of density along the *z*-axis, at the board mid-plane for different times after press closure

the gas escaping from the board edges, because the edge area is small when compared to the surface area. We also observe a slower rate of steam partial pressure rise at the surface layers. The effect of an external resistance for heat and mass transfer at board edges was previously studied (Carvalho 1999). For the range of external heat and mass transfer coefficients considered, only slight differences were observed on horizontal profiles of temperature and steam partial pressure near the board edges. We concluded that in the hot-pressing of MDF, the control of heat and mass transfer is internal. So, the results presented do not include an external heat and mass transfer resistance at the board edges.

These results should be considered qualitative rather than quantitative, since the estimation of many of the physical and mechanical parameters was done using correlations developed in different conditions, especially temperature range and materials (wood, particleboard, etc., Carvalho and Costa 1998).

Nevertheless, we next show a comparison between global model predictions and a few raw industrial data. These results concern the manufacture of boards with a final thickness of 19 mm (after sanding), having a thickness of about 21 mm at the end of the press cycle. The operating conditions are the same as described above, except for the platen temperature (195 °C) and the ambient temperature (21 °C). The press cycle time was 260 s.

In Fig. 3 we present a comparison between the board thickness schedule imposed on the simulations and the evolution of the top plate position in the

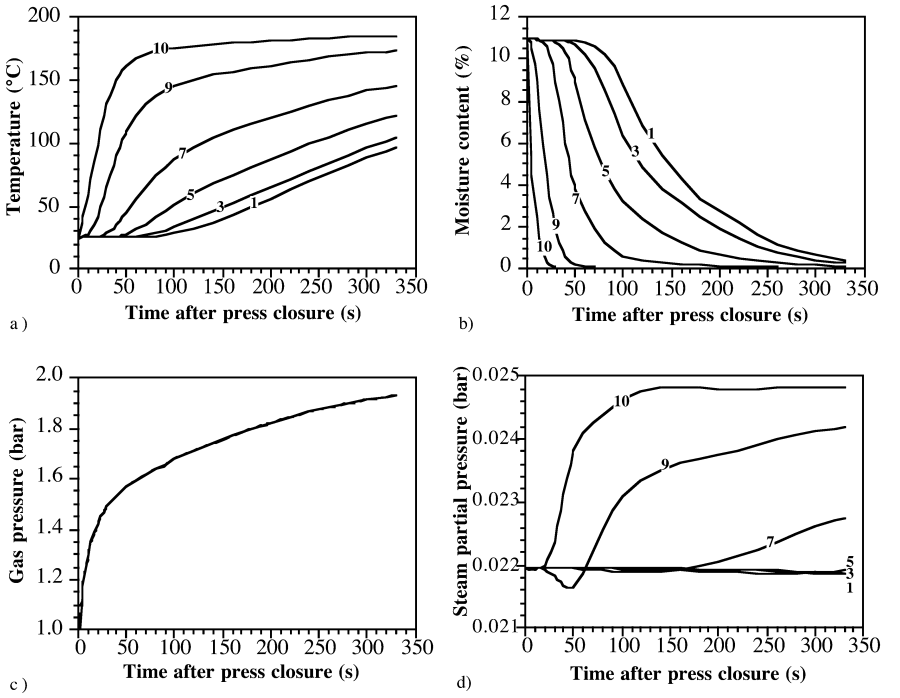

Fig. 2. Evolution of predicted **a** Temperature. **b** Moisture content. **c** Gas pressure. **d** Steam partial pressure along the *z*-axis at the central horizontal plane of the board with time after press closure for several positions in the vertical direction (*numbered from 1*, adjacent to board mid-plane, to *10*, adjacent to board surface

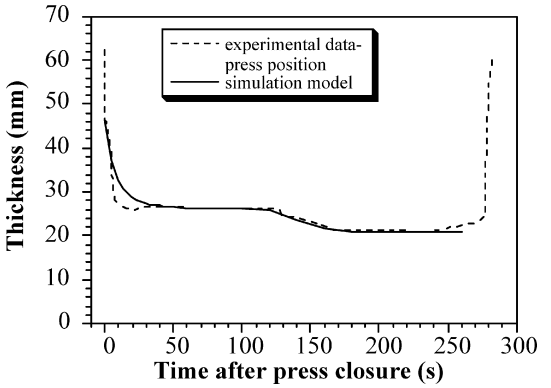

Fig. 3. Comparison between the board thickness schedule used to simulate the press cycle and the evolution of the superior platen press position of the industrial press

industrial press. In the simulations, the start-up press cycle thickness corresponds to the exact moment when the top plate touches the fiber mattress.

Figure 4 shows the experimental and simulated time evolution of the temperature at the center of the board. These experimental results were obtained by using a thermocouple positioned nearly at the board center.

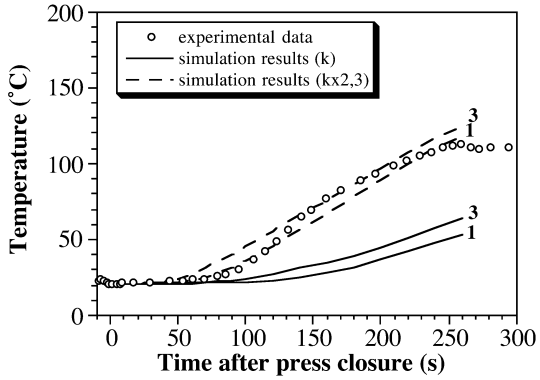

Fig. 4. Comparison between the observed evolution of temperature at the board center and the predicted evolution of temperature for two positions in the vertical direction (*numbered from 1*, adjacent to board mid-plane, to *10*, adjacent to board surface), considering for two board thermal conductivities

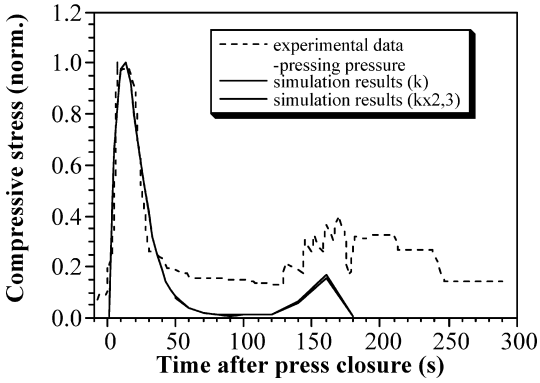

Fig. 5. Comparison between the evolution of pressure of the industrial press and the predicted evolution of overall compressive stress in response to a near step change in board thickness, for two board thermal conductivities

As we can see, the theoretical and experimental results are very different in magnitude. Several factors can cause this discrepancy, including the values of some physical parameters that were calculated using correlations for wood or particleboard. Such is the case for the thermal conductivity, which was estimated using an empirical correlation for particleboard. A sensitivity analysis was made, and it was verified that upon multiplying the thermal conductivity by a factor of 2.3, the results became very close. This factor leads to a value that is inside the range of the typical values for wood and wood-based panels (Siau 1984). This property is affected not only by the board structure, but also by local variables such as density and moisture content. So, the correction terms used for these variables, which were derived for particleboard and wood, may not be the most appropriate. On the other hand, the existence of preferential paths can lead to different resistances to heat transfer. Considering the three possible paths (air, water, cellular wall), the thermal conductivities are very different. From Siau (1984) the thermal conductivities (in W/mK) are equal to 0.024 for air, 0.691 for

water, 0.439 for the cellular wall in the direction normal to the grain and 0.877 for the cellular wall in direction parallel to the grain.

The total gas pressure, which is an important variable for press cycle control, was not analyzed because this variable is not measured in industry. In Fig. 5 we compare the evolution of the pressure of the industrial press with the model response in compressive stress.

The values are normalized because the effective pressure is unknown; only the pressure of the hydraulic system for each piston is known. A qualitative analysis shows that the model response is similar to the real one, although the model predicts a greater decrease in pressure after press closing, thus meaning that the relaxation of the real system is less than predicted. This can be overcome taking a higher value for the viscous component.

Finally, the model performance in predicting the physical and mechanical properties of the final product was studied. In Fig. 6 we can observe a comparison between the vertical density profile of an industrial board and the predicted density profile at the end of press cycle.

The experimental data was obtained using a γ-ray densitometer. We conclude that the predicted density profile for the corrected conductivity agrees both qualitatively and quantitatively with the experimental results. The mechanical performance of the final product is very important to its use. So, in the quality control of MDF several mechanical properties are considered, but the most important of these are the modulus of elasticity in bending, bending strength and the tensile strength perpendicular to the plane of the board. Unfortunately, direct comparison of these mechanical properties with those that can be predicted by the model is not possible. For this reason, we determined the modulus of elasticity in compression of several MDF specimens of size 50×50×16 mm. The tests were performed using a universal testing machine with a 50 kN load cell. A value of 59.7 MPa was obtained. Figure 7 shows the evolution of modulus of elasticity with time for the two values of thermal conductivity.

As can be seen, the experimental value is very close to those predicted by the model at the end of press cycle, although the closest value was obtained by using the corrected thermal conductivity. However, this value is lower than the experimental one, which was expected, because the MDF only attains its final resistance after a period of stabilization.

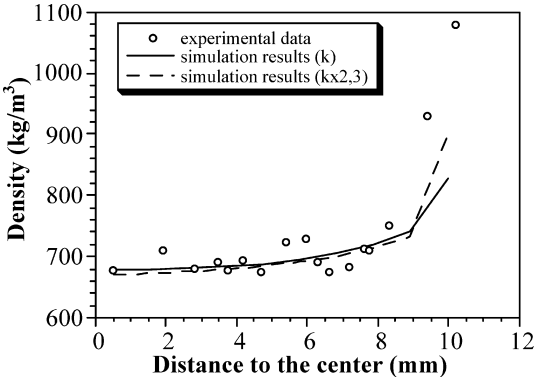

Fig. 6. Comparison between vertical density profile of the industrial board and predicted density profile at the end of press cycle, along the *z*-axis at the board midplane, for two board thermal conductivities

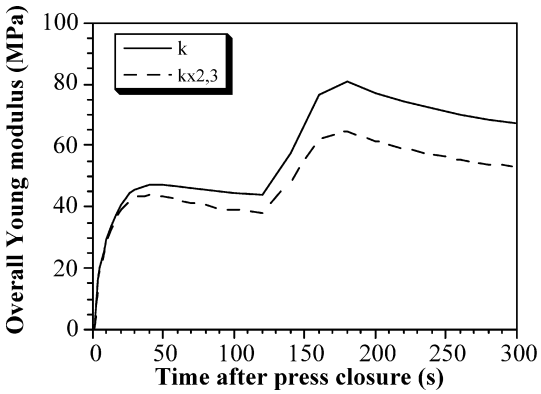

Fig. 7. Evolution of the overall Young's modulus with time after press closure for two board thermal conductivities

Conclusions

This paper presents a global model for the hot-pressing of MDF that integrates all mechanisms involved in the panel formation: heat and mass transfer, chemical reaction and mechanical behavior. The model performance was analyzed using typical operating conditions for the hot-pressing of MDF, and the parameters (physical, mechanical and transport properties) were calculated using the empirical and theoretical correlations from literature obtained for wood, particleboard or MDF. The kinetics of the UF cure reaction were derived using Raman spectroscopy. The global model was used to predict the evolution of the variables relating to heat and mass transfer (temperature, moisture content, gas pressure and relative humidity), as well as the variables relating to mechanical behavior (pressing pressure, strain, modulus of elasticity and density). The simulation results were important to identify the controlling factors of the hot-pressing operation, permitting us to better understand the complex mechanisms involved.

Finally, we attempt to compare the model prediction with the experimental data from an industrial MDF press. The available data permitted us to analyze the evolution of two dependent variables: temperature and compressive stress, and two mechanical properties: vertical density profile and modulus of elasticity in compression. The model can predict in an acceptable way the evolution of temperature at the board center during the press cycle if we take a higher value for the thermal conductivity. This correction is consistent with the fact that thermal conductivity was calculated with a correlation obtained for particleboard and not for MDF. The system response in compressive stress follows the evolution of the counterpressure of the industrial press, although the relaxation in the real system is less than predicted, which means that the viscous component should be higher. Concerning the physical–mechanical properties, the model is able to predict in a qualitative way the final vertical density profile of MDF as well as the modulus of elasticity in compression of this material.

However, the improvement of the model requires the accomplishment of an experimental program in a pilot-scale press in order to refine the model parameters. This will permit the scheduling of the press cycle to fulfill the objectives of minimization of energy consumption, better quality of the boards produced and increased process flexibility.

References

Carvalho LM, Costa C (1998) Modeling and simulation of the hot-pressing process in the production of medium density fiberboard (MDF). Chem Eng Comm 170:1–21

Carvalho LM, Costa CA (1997) Comparison between two- and three-dimensional models for heat and mass transfer in the hot-pressing process for MDF production. In: Proceedings of the 1st European congress on chemical engineering ECCE-1, vol 3, Firenze, Italy, pp 2129–2132

Carvalho LM, Costa MRN, Costa CA (2001) Modeling rheology in the hot-pressing of MDF: comparison of mechanical models. Wood Fiber Sci 33:395–411

Carvalho LMH (1999) Estudo da Operação de Prensagem do Aglomerado de Fibras de Média Densidade (MDF): Prensa Descontínua de Pratos Quentes. Dissertation, University of Porto, Portugal

Dai C, Steiner PR (1993) Compression behaviour of randomly formed wood flake mats. Wood Fiber Sci 25:349–358

De Boor C (1978) A practical guide to splines. Springer, Berlin Heidelberg New York

Gibson L, Ashby M (1988) Cellular solids: structure and properties. Pergamon, Oxford

Harless T, Wagner F, Short P, Seale D, Mitchell P, Ladd D (1987) A model to predict the density profile of particleboard. Wood Fiber Sci 19:81–92

Hata T, Kawai S, Sasaki H (1990) Computer simulation of temperature behavior in particle mat during hotpressing and steam injection pressing. Wood Sci Technol 24:65

Hindmarsh AC (1983) ODEPACK, a systematized collection of ODE solvers. In: RS Stepleman et al (eds) Scientific computing. North Holland, Amsterdam, pp 55–64

Humphrey P, Bolton AJ (1989) The hot pressing of dry formed wood-based composites. 2. Simulation model for heat and moisture transfer, and typical results. Holzforschung 43:199

Humphrey PE (1982) Physical aspects of wood particleboard manufacture. Dissertation, University of Wales, UK

Kamke FA, Wolcott MP (1991) Fundamentals of flakeboard manufacture: wood-moisture relationships. Wood Sci Technol 25:57

Kauman WG (1956) Equilibrium moisture content relations and drying control in superheated steam drying. For Prod J 6:328

Landau HG, Lewis RW (1950) Heat conduction in a melting solid. Q Appl Math 8:81–94

Lang EM, Wolcott MP (1996) A model for viscoelastic consolidation of wood-strand mats. 2. Static stress–strain behavior of the mat. Wood Fiber Sci 28:369–379

Lenth CA, Kamke FA (1996) Investigations of flakeboard mat consolidation. 2. Modeling mat consolidation using theories of cellular materials. Wood Fiber Sci 28:309–319

Maloney T (1989) Modern particleboard and dry-process fiberboard manufacturing. Miller Freeman, San Francisco

Patankar SV (1980) Numerical heat transfer and fluid flow. Hemisphere, New York

Siau JF (1984) Transport processes in wood. Springer, Berlin Heidelberg New York

Silva MA (2000) A general model for moving boundary problems—application to drying of porous media. Drying Technol 18:601–624

Suo S, Bowyer JL (1994) Simulation modeling of particleboard density profile. Wood Fiber Sci 26:397

Thoemen H, Humprey PE (1999) The continuous pressing process for wood-based panels: an analytical model. In: Proceedings of the third European panel products symposium, Llandudno, Wales, UK, pp 18–30

Yin S (1994) Caracterization par analyses thermiques de la polycondensation d'adhesives aminoplastes et du durcissement de composites modeles bois-adhesif. Dissertation, Université de Nancy I, France